

Predicting the FCI energy of large systems to chemical accuracy from restricted active space density matrix renormalization group calculations

Gero Friesecke,^{1,*} Gergely Barcza,² and Örs Legeza^{2,3,†}

¹*Department of Mathematics, Technical University of Munich, Germany*

²*Strongly Correlated Systems Lendület Research Group,*

Wigner Research Centre for Physics, H-1525, Budapest, Hungary

³*Institute for Advanced Study, Technical University of Munich, Germany, Lichtenbergstrasse 2a, 85748 Garching, Germany*

(Dated: September 29, 2022)

Abstract. We present a theoretical analysis and a new theory-based extrapolation method for the recently introduced restricted active space density matrix renormalization group (DMRG-RAS) method [arXiv:2111.06665] in electronic structure calculations. Large-scale numerical simulations show that our approach, DMRG-RAS-X, reaches chemical accuracy for challenging strongly correlated systems such as the Chromium dimer or dicarbon up to a large cc-pVQZ basis with moderate computational demands. The method is free of empirical parameters, performed robustly and reliably in all examples we tested, and has the potential to become a vital alternative method for electronic structure calculations in quantum chemistry, and more generally for the computation of strong correlations in nuclear and condensed matter physics.

I. INTRODUCTION

In light of tremendous progress in the past decade in transition metal chemistry [1–3], photosynthesis [4–7], single molecular magnets [8–10], and relativistic chemistry for compounds including heavy elements [11–15] the demand for a generally applicable method to efficiently treat strong electronic correlations and reveal solutions with chemical accuracy cannot be overemphasized. Although the main features of the electronic states are often characterized by the static correlations, contributions of an intractable number of high energy excited configurations with small weights, i.e., dynamical effects, can be crucial for an accurate theoretical description in light of experimental data [16, 17].

Quite recently, a cross-fertilization of the conventional restricted active space (RAS) scheme [18–22] with the density matrix renormalization group method [23, 24] via the dynamically extended active space procedure [25, 26] has emerged as a new powerful method [27] to capture both static and dynamic correlations, and numerical benchmarks on molecules with notorious multi-reference characters have revealed various advantages of the new method with respect to conventional approaches [21, 28–31].

It has also been demonstrated that the mapping of quantum lattice models to ab initio framework paves the road to attack challenging problems that are untractable by conventional approaches [32–34]. The dramatic reduction of entanglement for higher dimensional lattice models via fermionic mode transformation [35, 36] also makes the resulting ab initio problems excellent candidates for the DMRG-RAS method.

The observed very fast and robust convergence properties of the new method calls ultimately for a theoretical analysis in order to understand the underlying mechanisms and further improve the method. As has already been argued [27] and is elaborated below, the DMRG-RAS approach is a memory-efficient, Schmidt decomposition-based extension of the RAS scheme and it is an embedding method, in the sense that when orbitals are partitioned into two subspaces, CAS and EXT, the correlations between them are calculated self-consistently, in contrast to other post-DMRG approaches [37–44] which provide corrections on top of the DMRG wave function. In the DMRG-RAS procedure the excitation rank in the EXT subspace is truncated according to an a priori defined cutoff, inheriting the name RAS, while the eigenvalue equation for the many-body Hamiltonian defined on the tensor product space of the CAS and RAS is solved self-consistently by the usual DMRG procedure.

In this work, we present a theoretical analysis of the new method for the first time and introduce a new extrapolation procedure, free of empirical parameters and fully ab-initio, which reveals the ground state energy of systems with full Hilbert space dimensions up to 5×10^{16} within chemical accuracy (1 kcal/mole or 0.0016 a.u.). The principal insight is that the DMRG-RAS error rigorously is at most of the order of the square of the CAS error, and numerically exhibits stable power law scaling, allowing reliable extrapolation. We also show that DMRG-RAS is variational and exhibits monotone decay as the CAS-EXT split increases, unlike TCC where non-monotone behaviour is observed [45, 46]. The unique features of the new method, dubbed DMRG-RAS-X, are demonstrated via large scale calculations for various strongly correlated molecules up to a full orbital space with more than hundred orbitals. This is achieved by utilizing algorithmic progress developed in the past two decades based on concepts of quantum information

* gf@ma.tum.de

† legeza.ors@wigner.hu

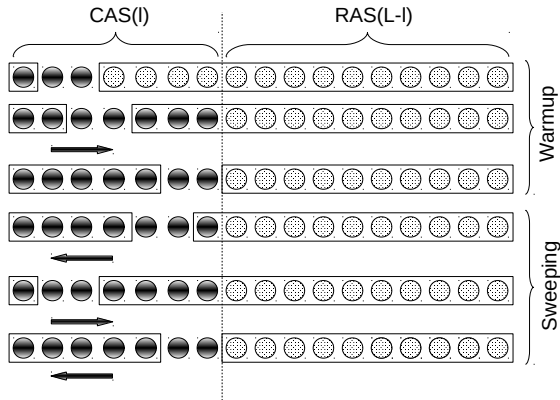


FIG. 1. Partitioning of the orbitals into ℓ CAS orbitals and $L - \ell$ RAS orbitals, with $N/2 \leq \ell \leq L$, in the DMRG-RAS method using the blocking structure introduced via the dynamically extended active space (DEAS) procedure. Filled circles stand for orbitals with four dimensional local Hilbert space, while orbital space built from dashed orbitals is restricted to an excitation threshold $k \leq N$. Arrows indicate the DMRG sweeping procedure and the vertical line shows the turning point of the forward sweep as the RAS orbitals are treated as a single site.

theory [47]. Therefore, our novel approach presented below, relying on a rigorous error scaling, can be applied to general systems and has the potential to become a widely used tool to target strongly correlated systems, in particular multi-reference problems in quantum chemistry[44, 47–51], nuclear structure theory [52–54] and condensed matter theory [55–57].

The setup of the paper is as follows. In Secs. II and III A we present the theory of the DMRG-RAS method, while in Secs. III B and III C we derive the error scaling for weakly interacting systems and general systems, respectively. In Sec. III D we introduce our new extrapolation method and in Sec. IV benchmark results obtained by large scale DMRG-RAS-X calculations are presented. Our work closes with main conclusions and future perspectives.

II. THE DMRG-RAS METHOD

The spinless single particle Hilbert space is spanned by L orthonormal orbitals $\varphi_1, \dots, \varphi_L \in L^2(\mathbb{R}^3)$, typically (but not necessarily) given by energy-ordered Hartree-Fock orbitals. In the DMRG-RAS method, one partitions the orbitals into ℓ CAS orbitals and $L - \ell$ RAS orbitals, with $N/2 \leq \ell \leq L$, and fixes an excitation threshold $k \leq N$, see Figure 1. The DMRG related blocking structure via the dynamically extended active space (DEAS) procedure will be described in more detail below. The

N -electron Hilbert space for the DMRG-RAS method is then given by

$$\mathcal{H}(\ell, k) = \mathcal{H}_{\text{CAS}}(\ell) \oplus \mathcal{H}_{\text{RAS}}(L - \ell, k)$$

where the CAS Hilbert space is the full N -electron Hilbert space of the CAS orbitals,

$$\mathcal{H}_{\text{CAS}} = \bigwedge_{i=1}^N \text{span}\{\varphi_1 \uparrow, \varphi_1 \downarrow, \dots, \varphi_\ell \uparrow, \varphi_\ell \downarrow\},$$

and the RAS Hilbert space is spanned by all Slater determinants which are at least singly and at most k -fold excited with respect to some CAS Slater determinant,

$$\mathcal{H}_{\text{RAS}} = a_{a_1 \sigma_1}^\dagger a_{j_1 \sigma_1'} \mathcal{H}_{\text{CAS}} \oplus \dots \oplus a_{a_1 \sigma_1}^\dagger \dots a_{a_k \sigma_k}^\dagger a_{j_1 \sigma_1'} \dots a_{j_k \sigma_k'} \mathcal{H}_{\text{CAS}}.$$

Here a and a^\dagger are the usual creation and annihilation operators, with CAS orbitals indexed by j_i , RAS orbitals indexed by a_i , and spin states indexed by σ_i, σ_i' . Thus the method has two parameters, ℓ (number of CAS orbitals) and k (RAS excitation threshold). While there is considerable freedom in choosing ℓ , the standard choice for k (and the one investigated in this paper) is $k = 2$.

Our interest is in the ground state energy $E^0 = E^0(\ell, k)$ and the ground state $\Psi^0 = \Psi^0(\ell, k)$ obtained from the Rayleigh-Ritz principle,

$$E^0(\ell, k) = \min_{\Psi \in \mathcal{H}(\ell, k): \langle \Psi, \Psi \rangle = 1} \langle \Psi, H \Psi \rangle, \quad (1)$$

where H is the (non-relativistic, Born-Oppenheimer) electronic Hamiltonian of the system, which can be written in second quantized form as

$$H = \sum_{ij\sigma} t_{ij\sigma} a_{i\sigma}^\dagger a_{j\sigma} + \frac{1}{2} \sum_{ijkl\sigma\sigma'} V_{ijkl} a_{i\sigma}^\dagger a_{j\sigma'}^\dagger a_{k\sigma'} a_{l\sigma}, \quad (2)$$

where t_{ij} denotes the matrix elements of the one-particle Hamiltonian, which is comprised of the kinetic energy and the external electric potential of the nuclei, and V_{ijkl} stands for the matrix elements of the electron repulsion operator. Replacing the Hilbert space in (1) by \mathcal{H}_{CAS} respectively $\mathcal{H}_{\text{CAS}} \oplus \mathcal{H}_{\text{RAS}}$ yields the CAS ground state energy and ground state $E_{\text{CAS}}^0(\ell), \Psi_{\text{CAS}}^0(\ell)$, respectively the RAS ground state energy and ground state $E_{\text{RAS}}^0(L - \ell, k), \Psi_{\text{RAS}}^0(L - \ell, k)$.

For a closed-shell system, Hartree-Fock orbitals, and the smallest choice of ℓ , i.e. $\ell = N/2$, the CAS Hilbert space is spanned by the Hartree-Fock determinant only. The CAS energy is then just the Hartree-Fock energy, and DMRG-RAS reduces to k -fold excited CI, i.e., when $k = 2$, to CISD. When $\ell > N/2$, DMRG-RAS is a multi-reference method.

We note also that for the largest (but typically unfeasible) choice $\ell = L$, the CAS energy $E_{CAS}^0(L)$ is the full configuration interaction (FCI) energy, regardless of the choice of orbitals. Likewise, for the largest choice $k = N$ of the excitation threshold the energy $E^0(\ell, N)$ again gives the FCI energy. Our central goal is a quantitative understanding of how accurately $E^0(\ell, k)$ captures the FCI energy.

In the numerical simulations, the DMRG-RAS calculations will be performed to obtain $E^0(\ell, 2)$ within a given error margin. In our implementation, we build on the dynamically extended active space (DEAS) procedure introduced two decades ago [25], where a multi-particle truncated Hilbert space is formed from a truncated set of one particle Hilbert spaces and DMRG right block auxiliary operators are calculated directly on that. A schematic picture of the partitioning of the ℓ CAS orbitals and $L - \ell$ RAS orbitals into the DMRG blocks through the forward and backward sweeping procedure is given in Fig. 1. For the warmup procedure, i.e., during the first forward sweep the right block is represented by the RAS space being equivalent to CISD for the CI-based truncated Hilbert space (CI-DEAS) [26, 47] until the size of the left block reaches the desired value of $\ell - 2$. In all subsequent sweeps, the usual DMRG optimization steps are carried out for the CAS orbital space and in the current implementation the RAS space is left intact, i.e., it is simply attached to the DMRG chain. We note that a similar procedure has been introduced recently in Ref. [58]. Using the dynamic block state selection (DBSS) approach [59, 60] with tight error margin it can be guaranteed that the error due to truncation in the DMRG procedure remains much smaller than that due to the Hilbert space truncation via a fixed RAS excitation threshold k .

III. THEORETICAL ANALYSIS

In this section, we provide the theoretical analysis of the DMRG-RAS method focusing on the scaling of the error as a function of ℓ , and we also introduce a new extrapolation method to improve significantly the prediction of the full-CI energy.

A. The reference Hamiltonian

A key step in predicting the accuracy of $E^0(\ell, k)$ is a judicious partitioning of the full Hamiltonian into a reference Hamiltonian associated with the CAS energy and a remainder. We propose the following choice:

$$H = H_0 + H' \text{ with} \quad (3)$$

$$H_0 = PHP + (E_0 + \Delta)Q \quad (4)$$

$$H' = H - PHP - (E_0 + \Delta)Q \quad (5)$$

where P is the projector of \mathcal{H} onto the CAS Hilbert space \mathcal{H}_{CAS} , $Q = I - P$ is the projector onto the RAS Hilbert

space, E_0 is the CAS ground state energy, i.e.

$$E_0 = E_{CAS}^0(\ell), \quad (6)$$

and $\Delta > 0$ is a parameter to be chosen later. This partitioning has the following desirable features:

(i) The CAS ground state energy is the ground state energy of H_0 (this is guaranteed by eqs. (4) and (6) and the positivity of Δ);

(ii) The operator $H_0 - E_0$ is invertible on the orthogonal complement of the ground state of H_0 , yielding well-defined perturbation corrections at all orders;

(iii) the first order perturbation correction $E^{(1)} = \langle \Psi_0 | H' | \Psi_0 \rangle$ vanishes regardless of the choice of the orbitals and parameters such as ℓ and Δ ;

(iv) H_0 does not couple the CAS and RAS Hilbert spaces, with all the coupling contained in H' .

The latter property is evident by re-writing

$$H - PHP = \underbrace{QHP}_{\mathcal{H}_{CAS} \rightarrow \mathcal{H}_{RAS}} + \underbrace{PHQ}_{\mathcal{H}_{RAS} \rightarrow \mathcal{H}_{CAS}} + \underbrace{QHQ}_{\mathcal{H}_{RAS} \rightarrow \mathcal{H}_{RAS}}$$

(where the first term maps CAS to RAS, the second one, RAS to CAS, and the last one, RAS to itself), and makes transparent that DMRG-RAS can be considered an *embedding method*.

The above partitioning is by no means the only one that achieves properties (i)–(iv), but it is perhaps the simplest, and allows to accurately predict the FCI energy, as shown below.

B. Error scaling for weakly interacting systems

It is instructive to first discuss the case when H' is small. So let us introduce a coupling constant $\lambda > 0$ and look at the ground state energy $E_\lambda(\ell, k)$ of

$$H_0 + \lambda H' \quad (7)$$

on $\mathcal{H}(\ell, k)$ for small λ . We focus on the standard choice $k = 2$. This energy shall be compared to the FCI energy $E_\lambda^{\text{FCI}} = E_\lambda(\ell, N)$.

Recall the reduced resolvent R_0 of H_0 ,

$$R_0 = \begin{cases} 0 & \text{on the ground state of } H_0 \\ (H_0 - E_0)^{-1} & \text{on (ground state)}^\perp \end{cases}$$

where (ground state) $^\perp$ denotes the orthogonal complement of the ground state within the full Hilbert space $\mathcal{H}(\ell, k)$. In theoretical discussions of perturbation theory, the reduced resolvent is often expressed in terms of the excited eigenvalues and eigenstates of H_0 as $R_0 = \sum_{n \neq 0} (E_n - E_0)^{-1} |\Psi_n\rangle \langle \Psi_n|$; but this information is neither needed for our purposes, nor available in practice in cases like ours when H_0 is a many-body operator.

By standard Rayleigh-Schrödinger perturbation theory (see e.g. [61]), assuming the ground state of H_0 is nondegenerate and denoting it by Ψ_0 ,

$$E_\lambda^{\text{FCI}} = E_0 + \lambda E^{(1)} + \lambda^2 E^{(2)} + \lambda^3 E^{(3)} + O(\lambda^4) \quad (8)$$

as $\lambda \rightarrow 0$, with

$$E^{(1)} = \langle \Psi_0 | H' | \Psi_0 \rangle, \quad (9)$$

$$E^{(2)} = \langle \Psi_0 | H' | \Psi^{(1)} \rangle \\ = -\langle \Psi_0 | H' R_0 H' | \Psi_0 \rangle, \quad (10)$$

$$E^{(3)} = \langle \Psi_0 | H' R_0 (H' - E^{(1)}) R_0 H' | \Psi_0 \rangle \\ = \langle \Psi^{(1)} | H' - E^{(1)} | \Psi^{(1)} \rangle. \quad (11)$$

Here

$$\Psi^{(1)} = -R_0 H' \Psi_0 \quad (12)$$

is the first order wavefunction correction under the standard normalization $\langle \Psi_0 | \Psi_\lambda^{\text{FCI}} \rangle = 1$, so that

$$\Psi_\lambda^{\text{FCI}} = \Psi_0 + \lambda \Psi^{(1)} + O(\lambda^2) \quad (13)$$

as $\lambda \rightarrow 0$.

We now investigate the DMRG-RAS energy with excitation threshold $k = 2$, i.e., $E_\lambda(\ell, 2)$. The key point is that, in our case,

$$\Psi^{(1)} = -R_0 H' \Psi_0 \in \mathcal{H}_{\text{CAS}}(\ell) \oplus \mathcal{H}_{\text{RAS}}(L - \ell, 2).$$

This is because (i) H is a two-body operator, so it maps Ψ_0 into $\mathcal{H}_{\text{CAS}}(\ell) \oplus \mathcal{H}_{\text{RAS}}(L - \ell, 2)$, (ii) R_0 is, by eq. (4), a zero-body operator (i.e. a multiple of the identity) on $\mathcal{H}_{\text{RAS}}(L - \ell, 2)$. Hence $(\Psi_0 + \lambda \Psi^{(1)}) / \|\Psi_0 + \lambda \Psi^{(1)}\|$ is an admissible trial function in the variational principle for $E_\lambda(\ell, 2)$, giving

$$E_\lambda(\ell, 2) \leq \frac{\langle \Psi_0 + \lambda \Psi^{(1)} | H_0 + \lambda H' | \Psi_0 + \lambda \Psi^{(1)} \rangle}{1 + \lambda^2 \|\Psi^{(1)}\|^2} \quad (14)$$

$$= E_0 + \frac{\lambda E^{(1)} + \lambda^2 E^{(2)} + \lambda^3 \langle \Psi^{(1)} | H' | \Psi^{(1)} \rangle}{1 + \lambda^2 \|\Psi^{(1)}\|^2}. \quad (15)$$

Here the last expression follows by multiplying out the numerator in (14), re-writing the term $\lambda^2 \langle \Psi^{(1)} | H_0 | \Psi^{(1)} \rangle$ as $\lambda^2 E_0 \|\Psi^{(1)}\|^2 + \lambda^2 \langle \Psi^{(1)} | H_0 - E_0 | \Psi^{(1)} \rangle$, and using that

$$\langle \Psi^{(1)} | H_0 - E_0 | \Psi^{(1)} \rangle = -E^{(2)}$$

(since $(H_0 - E_0)R_0$ is the identity on the orthogonal complement of Ψ_0 , to which $H' \Psi_0$ belongs).

By Taylor-expanding 1 over the denominator as $1 - \lambda^2 \|\Psi^{(1)}\|^2 + O(\lambda^4)$,

$$E_\lambda(\ell, 2) \leq E_0 + \lambda E^{(1)} + \lambda^2 E^{(2)} + \lambda^3 E^{(3)} + O(\lambda^4),$$

matching the expansion of the FCI energy to $O(\lambda^4)$. Together with the trivial lower bound $E_\lambda(\ell, 2) \geq E_\lambda^{\text{FCI}}$ this yields the overall error scaling

$$e_\lambda^{\text{RAS}} = E_\lambda(\ell, 2) - E_\lambda^{\text{FCI}} = O(\lambda^4) \text{ as } \lambda \rightarrow 0. \quad (16)$$

On the other hand, since $E^{(1)} = 0$ and $E^{(2)} < 0$, the pure CAS error satisfies

$$e_\lambda^{\text{CAS}} = E_0 - E_\lambda^{\text{FCI}} = \Omega(\lambda^2) \text{ as } \lambda \rightarrow 0. \quad (17)$$

Here the Landau symbol $\Omega(\lambda^p)$ denotes any term which stays bounded from below by a positive constant times λ^p (analogously to the more common Landau symbol $O(\lambda^p)$ which denotes any term bounded above by a positive constant times λ^p). Combining with (16) gives the following scaling law which relates the CAS and DMRG-RAS error:

$$e_\lambda^{\text{RAS}} = O\left((e_\lambda^{\text{CAS}})^2\right) \text{ as } \lambda \rightarrow 0. \quad (18)$$

C. Error scaling for general systems

Predictions of Rayleigh-Schrödinger perturbation theory have to be viewed with some caution, here and in many other cases (eq. (16), Moller-Plesset perturbation theory, Görling-Levy perturbation theory, ...). The reason is that the perturbing operator H' , which describes the action of the original Hamiltonian on omitted pieces of the Hilbert space and between kept and omitted pieces, is not small, in the sense of smallness of its matrix elements $\langle \Psi | H' | \Phi \rangle$ or its operator norm

$$\|H'\| = \max_{\|\Psi\|=1} \|H'\Psi\| = \max_{\|\Psi\|=\|\Phi\|=1} |\langle \Psi | H' | \Phi \rangle|. \quad (19)$$

But the small parameter λ in classical RS perturbation theory is precisely the operator norm $\|H'\|$ (as seen from writing $H' = \lambda \tilde{H}'$ with the fixed operator $\tilde{H}' = H' / \|H'\|$). To summarize: neglecting higher-order energy contributions is rigorously justified only when $\|H'\|$ is small; but this condition is not met in practice.

What *can* be made small in practice in the DMRG-RAS method, by increasing the number ℓ of CAS orbitals to a reasonable value, is the *action of the perturbation operator H' on the CAS ground state*,

$$\|H'\Psi_0\|. \quad (20)$$

This quantity measures the total size of the Slater determinants in the RAS Hilbert space which get activated by applying the full Hamiltonian to the CAS ground state. (The actual ℓ needed to make this quantity small depends on the system. Of course, a weakly correlated system can be captured sufficiently well by a small number of active orbitals, whereas a significantly larger ℓ is required for strongly correlated systems; see the numerical results below.) We believe the scaling laws (16), (17), (18) to remain approximately correct when only (20) (instead of (19)) is small.

In the following we offer a theoretical argument in support of this claim. Thus we aim to estimate the CAS and DMRG-RAS error at the physical value $\lambda = 1$ in (7), in terms of $\|H'\Psi_0\|$. We start from the variational upper bound (15), which is valid for any λ , and use the explicit form of H_0 and H' to simplify. Recalling the notation $H_{\text{CAS} \rightarrow \text{RAS}}$ for the ‘‘off-diagonal’’ block QHP of the Hamiltonian which maps CAS to RAS and abbreviating

$$\Psi' = H'\Psi_0 = H_{\text{CAS} \rightarrow \text{RAS}} \Psi_0, \quad (21)$$

we obtain

$$\begin{aligned} E^{(1)} &= 0, \\ \Psi^{(1)} &= -\Delta^{-1}\Psi', \\ E^{(2)} &= -\Delta^{-1}\|\Psi'\|^2, \\ \langle \Psi^{(1)} | H' | \Psi^{(1)} \rangle &= \Delta^{-2} \langle \Psi' | (H_{\text{RAS}} - E_0) - \Delta | \Psi' \rangle. \end{aligned} \quad (22)$$

Note also that, because $E^{(1)} = 0$, in our case we have

$$\langle \Psi^{(1)} | H' | \Psi^{(1)} \rangle = E^{(3)}. \quad (23)$$

Setting $\lambda = 1$ now gives the following upper bound for the DMRG-RAS energy:

$$\begin{aligned} E^0(\ell, 2) - E_0 &\leq \frac{-\Delta^{-1}\|\Psi'\|^2 + \Delta^{-2} \langle \Psi' | (H_{\text{RAS}} - E_0) - \Delta | \Psi' \rangle}{1 + \Delta^{-2}\|\Psi'\|^2} \\ &= \frac{-2\Delta^{-1}\|\Psi'\|^2 + \Delta^{-2} \langle \Psi' | H_{\text{RAS}} - E_0 | \Psi' \rangle}{1 + \Delta^{-2}\|\Psi'\|^2}. \end{aligned}$$

We now exploit the freedom of choosing Δ , and minimize the numerator with respect to Δ . (One could instead optimize the whole right hand side, but this would not lead to a notable quantitative improvement, and lose the simple structure and physical interpretability of the result below.) The elementary calculus problem of minimizing $h(\Delta) = -2\Delta^{-1}a + \Delta^{-2}b$ for given $a, b > 0$ is solved by $\Delta = \frac{b}{a}$, giving a minimum value of $-\Delta^{-1}a$. Consequently, provided

$$\langle \Psi' | H_{\text{RAS}} - E_0 | \Psi' \rangle > 0 \quad (24)$$

we set

$$\Delta = \frac{\langle \Psi' | H_{\text{RAS}} - E_0 | \Psi' \rangle}{\|\Psi'\|^2} \quad (25)$$

and obtain, for this choice of Δ ,

$$E^0(\ell, 2) \leq E_0 - \frac{\Delta^{-1}\|\Psi'\|^2}{1 + \Delta^{-2}\|\Psi'\|^2}. \quad (26)$$

This inequality is the key technical result of this section. Remembering that $\|\Psi'\| = \|H'\Psi_0\|$, it says that the CAS error contains a quadratic term in $\|H'\Psi_0\|^2$, and that the DMRG-RAS method removes it. Which analog of (16), (17), (18) does this imply?

First, immediately from (26) and the trivial fact $E_{\text{FCI}} \leq E^0(\ell, 2)$, the CAS error satisfies

$$\begin{aligned} \epsilon_{\text{CAS}}(\ell) &= E_0 - E_{\text{FCI}} \leq E_0 - E^0(\ell, 2) \\ &= \Omega(\|H'\Psi_0\|^2) \text{ as } \|H'\Psi_0\| \rightarrow 0. \end{aligned} \quad (27)$$

Second, while we cannot offer a rigorous proof that the DMRG-RAS error is quartic in $\|H'\Psi_0\|$, we obtain the following interesting result in this direction:

$$\begin{aligned} E^0(\ell, 2) - (E_0 + E^{(1)} + E^{(2)} + E^{(3)}) &\leq O(\|H'\Psi_0\|^4) \\ &\text{as } \|H'\Psi_0\| \rightarrow 0. \end{aligned} \quad (28)$$

Without the $E^{(3)}$ term, this follows from (26), the Taylor expansion $1/(1+\Delta^{-2}\|\Psi'\|^2) = 1 - \Delta^{-2}\|\Psi'\|^2 + O(\|\Psi'\|^4)$, and the first and third formula in (22). But, remarkably, the optimal Δ (eq. (25), obtained here from nonperturbative considerations) makes the third order perturbation correction $E^{(3)}$ vanish, as is seen from the last formula in (22).

The important advance of (28)–(27) over (16)–(17) is that the error is now quantified in powers of (20) not (19), which is needed for applicability to realistic systems. Eqs. (27)–(28) make us expect

$$\epsilon_{\text{RAS}} = O\left(\epsilon_{\text{CAS}}^2\right) \text{ as } \|H'\Psi_0\| \rightarrow 0 \quad (29)$$

where $\epsilon_{\text{RAS}} = E^0(\ell, 2) - E_{\text{FCI}}$ is the DMRG-RAS error. Since the CAS error decays monotonically to zero as the number ℓ of CAS orbitals increases, this means that – as soon as ℓ is large enough – the RAS error decays to zero much faster.

Finally let us physically interpret the condition (24) and the formula (25) underlying these results.

The optimal Δ defined by (25) is the *expected value of the spectral gap between the pure RAS eigenvalues and the CAS ground state* with respect to the particular RAS state $\Psi'/\|\Psi'\|$. It thus indicates the typical gap between energy levels into which the full Hamiltonian promotes the CAS ground state, and the CAS ground state energy. In particular, Δ does not depend on the spectral gap between ground and first excited state within the CAS, and is lower-bounded by the spectral gap

$$\begin{aligned} \Delta_{\min} &= \text{lowest eigenvalue of } H_{\text{CAS}} \\ &\quad - \text{lowest eigenvalue of } H_{\text{RAS}} \end{aligned}$$

between the pure RAS and pure CAS ground state energies.

Eq. (24) simply says that the expected value of the RAS Hamiltonian H_{RAS} on the state $\Psi'/\|\Psi'\|$ is bigger than the CAS ground state energy E_0 (or equivalently, that $\Delta > 0$). Clearly, since Ψ' lies in \mathcal{H}_{RAS} , a sufficient condition for (24) is that the ground state energy purely on \mathcal{H}_{RAS} is bigger than that purely on \mathcal{H}_{CAS} (or equivalently, that $\Delta_{\min} > 0$). This is a minimal (and in practice never violated) restriction on the choice of CAS and RAS orbitals.

D. New extrapolation method

Suppose we have numerically calculated the CAS energy $E_{\text{CAS}}^0(\ell)$ and the DMRG-RAS energy $E^0(\ell, 2)$ for a few values of ℓ . The scaling law (29) now gives some information about the (unknown) FCI energy, namely

$$E^0(\ell, 2) - E^{\text{FCI}} \leq a(E_{\text{CAS}}^0(\ell) - E^{\text{FCI}})^2$$

for some constant a which does not depend on ℓ . In practice the DMRG-RAS method performs even better.

Its error is numerically observed in our examples to scale like a power of the CAS error, but the power is bigger than 2. That is to say, we observe a scaling law of the semi-empirical form

$$E^0(\ell, 2) - E^{\text{FCI}} = a(E_{\text{CAS}}^0(\ell) - E^{\text{FCI}})^p \text{ for some } p > 2. \quad (30)$$

See the numerical results in the next section. We trace this to the fact that DMRG-RAS is a fully self-consistent method, and therefore capable of capturing more than the guaranteed perturbation contributions. Also, the fact that both H_0 and H' are changing with ℓ is likely to play a role. Further theoretical investigation lies beyond our scope.

The main corollary of our analysis, relying on the validity of Eq. 30, is to provide a new extrapolation method to estimate the full-CI energy within chemical accuracy from an available $E_{\text{CAS}}^0(\ell)$ and $E^0(\ell, 2)$ data set. Equivalently, our goal is to predict the exponent p , the prefactor a and the offset E_{FCI} from $E_{\text{CAS}}^0(\ell)$ and $E^0(\ell, 2) = E_{\text{RAS}}(\ell)$. This is achieved by minimizing the mean squared regression error of RAS versus CAS error in a log log plot,

$$\text{MSE} = \frac{1}{n} \sum_{\ell} \left(y_{\ell} - (p \cdot x_{\ell} + \log a) \right)^2 \quad (31)$$

where n is the number of datapoints and

$$x_{\ell} = \log(E_{\text{CAS}}(\ell) - E_{\text{FCI}}), \quad y_{\ell} = \log(E_{\text{RAS}}(\ell) - E_{\text{FCI}}). \quad (32)$$

Vanishing of the regression error (31) corresponds to exact validity of the scaling law (30). The minimization over the prefactor a and the exponent p can be carried out explicitly, yielding

$$p_{\text{RAS-X}} = \frac{\sum_{\ell} (y_{\ell} - \bar{y})(x_{\ell} - \bar{x})}{\sum_{\ell} (x_{\ell} - \bar{x})^2}, \quad \log a_{\text{RAS-X}} = \bar{y} - p_{\text{RAS-X}} \bar{x} \quad (33)$$

where \bar{x} , \bar{y} are the average values of x_{ℓ} and y_{ℓ} . This reduces the minimization of (31) to a numerical minimization over the single free variable E_{FCI} . The predicted FCI energy is then

$$E_{\text{RAS-X}} = \arg \min_{E_{\text{FCI}}} \text{MSE}, \quad \text{MSE given by (31)-(33)}.$$

IV. NUMERICAL RESULTS

In this section we provide numerical justification for the theory presented in the previous section, focusing on the prediction given by Eq. 30. Here, let us remark that the overall error of the DMRG-RAS method stems from three main sources: (a) the split of the full orbital space to CAS and RAS parts; (b) the truncation of the RAS part based on k ; and (c) the error of the DMRG used to approximate the CAS part. The latter one can be controlled using the dynamic block state selection (DBBS)

approach [25, 60] to stay below an a priori defined error threshold, χ . The truncation on the RAS part is fixed by choosing $k = 2$. Therefore, the main question to be answered is the error dependence on ℓ . We remark here that the ℓ -dependence hinges on a good choice of the CAS space and on the chosen basis [27, 62]. Since orbitals lying close to the Fermi surface possess the largest one-orbital entropies [25], a selection based on orbital entropy together with keeping the almost fully occupied orbitals in the CAS space is an efficient protocol [25, 46, 63].

Let us also note that a very accurate extrapolation procedure requires to perform CAS and DMRG-RAS calculations for various χ values for each ℓ in order to perform an extrapolation to the DMRG truncation free limit, i.e., to obtain $E^0(\ell) = \lim_{\chi \rightarrow 0} E_{\chi}^0(\ell)$ and $E^0(\ell, k) = \lim_{\chi \rightarrow 0} E_{\chi}^0(\ell, k)$. In this work, we have not performed this step since both ε_{CAS} and ε_{RAS} were found to be larger by at least one order magnitude than χ for the accessed ℓ values and for the systems studied below.

A. Numerical justification of the error prediction from theory

First we investigate smaller systems with full-CI Hilbert space dimension not exceeding 10^{10} , so that exact diagonalization can be carried out and the full-CI energy is available.

In Fig. 2 we consider the CH_2 molecule. The absolute error of the DMRG-RAS ground state energy, $\varepsilon(\ell)_{\text{RAS}}$, is plotted as a function of the absolute error of the CAS ground state energy, $\varepsilon(\ell)_{\text{CAS}}$, on a double logarithmic scale, using the split valence basis. In the full orbital space this describes the correlation of 6 electrons on 12 (spatial) orbitals, i.e., CAS(6,12) with $\dim \mathcal{H}_{\text{FCI}} \approx 1.3 \times 10^5$. In order to acquire numerically exact data we have set the DMRG bond dimension to $D = 16384$ and the residual error of the Davidson diagonalization method to $\varepsilon_{\text{Davidson}} = 10^{-11}$. It is clearly seen in the figure that data points for increasing ℓ values fall on a line on the double logarithmic scale. This justifies the prediction of Eq. 30. In fact the fitted exponent comes out as $p_{\text{fit}} = 2.09$, a value that is very close to the upper bound given by perturbation theory.

Next, we consider the F_2 molecule at $d = 2.68797a_0$ in the basis of split valence orbitals [64] corresponding to CAS(18,18) with $\dim \mathcal{H}_{\text{FCI}} \approx 9 \times 10^9$ which is almost the limit for exact diagonalization. Here, DMRG was performed using the DBSS procedure by setting $D_{\text{min}} = 2048$, $D_{\text{max}} = 15000$, and both the quantum information loss χ and $\varepsilon_{\text{Davidson}}$ to 10^{-6} . The full-CI energy was taken from Ref. [59]. Again data points lie along a line and the fitted value $p_{\text{fit}} = 3.12$ indicates that important corrections beyond perturbation theory are captured.

Turning towards much larger systems and with more pronounced correlations, i.e., to multi-reference problems, we show results for the N_2 molecule at inter molecular distance $d = 2.118a_0$ in the cc-pVDZ basis and for

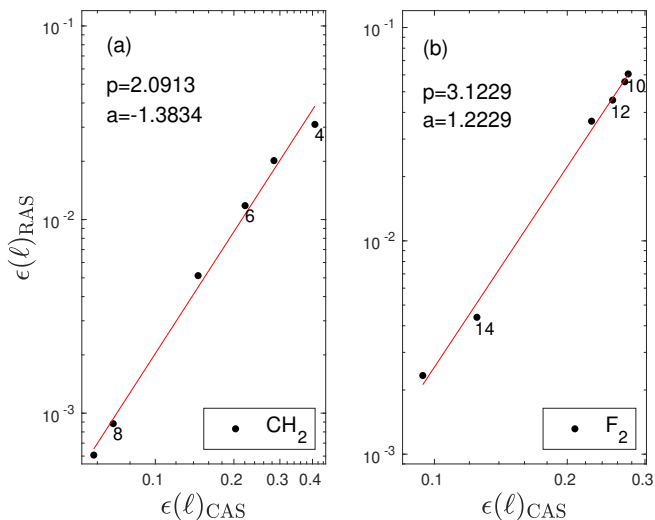


FIG. 2. (a) $\varepsilon(\ell)_{\text{RAS}}$ as a function of $\varepsilon(\ell)_{\text{CAS}}$ shown on a double logarithmic scale for the CH_2 molecule in the split valence basis corresponding to CAS(6,12). The solid line is a fit according to Eq. 30 and the obtained values for p_{fit} and a_{fit} are also shown. Labels next to data points stand for values of ℓ . (b) Similar to (a) but for the F_2 molecule at $d = 2.68797a_0$ using the basis of split valence orbitals corresponding to CAS(18,18).

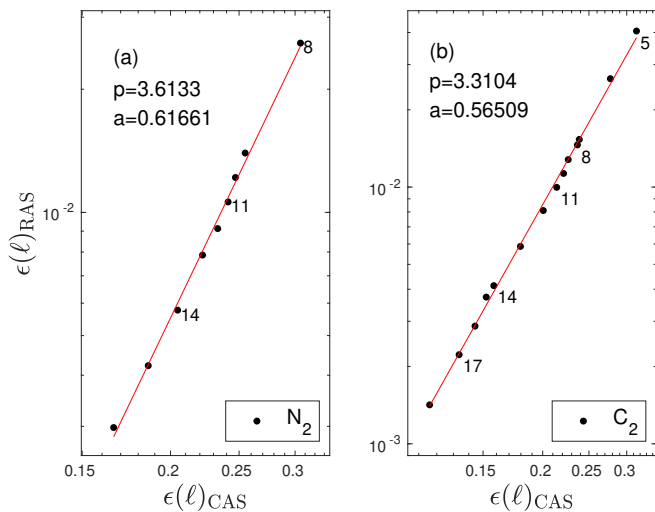


FIG. 3. (a) Similar to Fig. 2 but for the N_2 molecule at $d = 2.118a_0$ in the cc-pVDZ basis corresponding to CAS(14,28). (b) Similar to (a) but for the C_2 molecule at $d = 1.25\text{\AA}$ in the frozen core cc-pVTZ basis corresponding to CAS(8,58).

the C_2 molecule at $d = 1.25\text{\AA}$, in the frozen core cc-pVTZ basis [65], i.e., for CAS(14,28) with $\dim \mathcal{H}_{\text{FCI}} \approx 5.8 \times 10^{12}$ and CAS(8,58) with $\dim \mathcal{H}_{\text{FCI}} \approx 6.3 \times 10^{11}$, respectively. In both cases, the same numerical settings have been applied as for F_2 . The numerically estimated full-CI ground state energy was taken from Ref. [46] and from [27], respectively. The data show near-perfect agreement with the behavior predicted from theory, and the slopes of the fits are $p_{\text{fit}} = 3.6$ and 3.3, respectively. Therefore, we can

system	ε_{CAS}	ε_{RAS}	$\varepsilon_{\text{RAS-X}}$	L/ℓ_{max}	$\varepsilon_{\text{RAS-X}}/\varepsilon_{\text{RAS}}$
F_2	0.0941	0.0023	0.0011	1.20	0.48
CH_2	0.0690	0.0009	-0.0004	1.33	0.29
N_2	0.1662	0.0030	0.0007	1.75	0.23
C_2	0.1159	0.0014	0.0001	3.22	0.07

TABLE I. Absolute error of the ground state energy for various systems, for the CAS, RAS, and RAS-X method. For the first two methods we used the largest ℓ values (i.e. the maximal number of CAS orbitals, ℓ_{max}) in Figures 2 and 3. Also shown: ratio L/ℓ_{max} of total number of orbitals to maximal number of CAS orbitals, and ratio of RAS-X to RAS error.

conclude that the power law scaling in eq. 30 holds for realistic systems.

B. Numerically predicting the FCI energy within chemical accuracy

We now demonstrate that the new extrapolation method presented in Sec. IIID by Eq. 30 can be applied to realistic systems, providing both the ground state energy within chemical accuracy and an intrinsic error estimate for the DMRG-RAS calculation which does not require external reference data. In Fig. 4 the result of this minimization procedure providing $p_{\text{RAS-X}}$ and $E_{\text{RAS-X}}$ is presented for CH_2 , F_2 , N_2 and C_2 . The predicted exponents are in all cases close to the fitted values obtained by using corresponding Full-CI reference energies (see Figs. 2 and 3); in fact, in case of C_2 , the difference is of the order of 10^{-2} . More importantly, the extrapolation reduces the absolute error in the ground state energies significantly. The lowest values of the absolute error in the ground state energy achieved at the largest values of ℓ for the CAS and RAS methods, together with extrapolated values, are summarized in Tab. I. Our numerical data demonstrate that the absolute error is reduced by one to two orders of magnitude by the DMRG-RAS method with respect to the restricted CAS space solution, and it is further reduced by a factor of 2 to 15 via the new extrapolation procedure according to Eq. 30. This further reduction in error becomes monotonically better as the ratio L/ℓ_{max} of total number of orbitals to maximal number of CAS orbitals increases, as is seen from the last two columns of the table. In addition, the difference between E_{RAS} and $E_{\text{RAS-X}}$ provides an estimate the error of a DMRG-RAS calculation without reference to external data, which is a unique and in our opinion very important feature among methods developed for electronic structure calculations.

As a final test we have repeated our analysis for stretched geometries of N_2 , i.e. for bond lengths $d = 2.700a_0$ and $3.600a_0$. By increasing d the multi reference character of the wave function, i.e., the contribution of dynamic correlations, becomes more pronounced. In Table. II the DMRG and CC energies obtained for the full

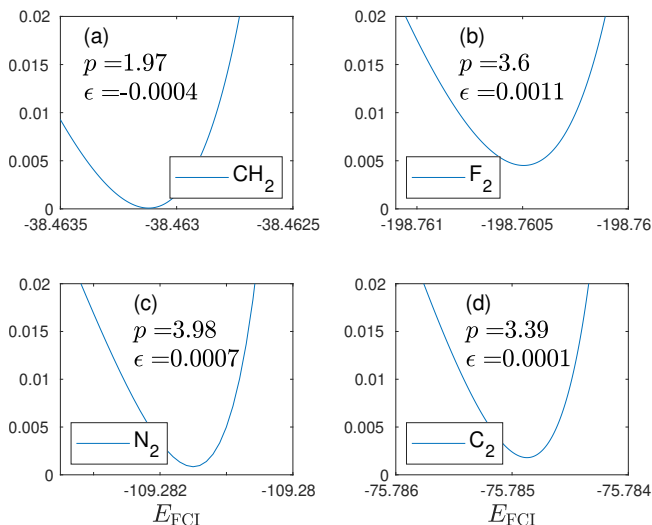


FIG. 4. (a),(b),(c) and (d) show the regression error, Eq. (31), as a function of E_{FCI} for the CH_2 , F_2 , N_2 , and for the C_2 molecules, respectively, at the predicted value $p_{\text{RAS-X}}$ of the exponent. The latter, and the absolute error $\epsilon_{\text{RAS-X}}$ given by the predicted value of E_{FCI} minus the full-CI energy, are also included.

	$d = 2.118a_0$	$d = 2.700a_0$	$d = 3.600a_0$
E_{CCSD}	-109.26762	-109.13166	-108.92531
E_{CCSDT}	-109.28032	-109.15675	-109.01408
E_{CCDTQ}	-109.28194	-109.16224	-108.99752
$E_{\text{RAS-X}}$	-109.2814	-109.1634	-108.9980
$p_{\text{RAS-X}}$	3.98	3.45	3.23
$\epsilon_{\text{RAS-X}}$	0.0007	0.0002	0.0001
p_{fit}	3.61	3.34	3.20
E_{DMRG}	-109.282165	-109.16359	-108.99807

TABLE II. Full-CI ground state energies obtained by large-scale DMRG calculations with $M_{\text{min}} = 1024$, $M_{\text{max}} = 10000$ and $\chi = 10^{-6}$, together with CC reference energies taken from Ref. [46] and predicted values $E_{\text{RAS-X}}$, $p_{\text{RAS-X}}$ and $\epsilon_{\text{RAS-X}}$ via the DMRG-RAS-X method using $\ell = 8 \dots 16$ for various bond lengths for the N_2 dimer in the cc-pVDZ basis. The p_{fit} values correspond to direct fits of ϵ_{RAS} vs ϵ_{CAS} as shown in Fig. 3 using the full-CI reference energies.

orbital space, together with extrapolated full-CI energies, $E_{\text{RAS-X}}$ and related exponents $p_{\text{RAS-X}}$ using $\ell = 8 \dots 16$ are summarized. Values of p_{fit} obtained by direct fits of ϵ_{RAS} vs ϵ_{CAS} using the full-CI reference energies, as shown in Fig. 3, are also included for comparison. Our result confirms that the DMRG-RAS-X method provides very accurate energy values not only for equilibrium geometries but also in situations when dynamic correlations are even more pronounced.

C. Results for large basis sets and the stability of the DMRG-RAS-X method

In this section, we present our results for larger systems and larger basis sets. For such systems the full-CI energy is not available, so our DMRG-RAS and DMRG-RAS-X results can only be compared to calculations performed with conventional methods like CC or MRCI, or to reference data accessible in the literature.

First, we show our result for the notoriously strongly correlated chromium dimer which is subject to usual benchmark calculations even nowadays [27, 38, 40, 66–68]. Our result for Cr_2 in a natural orbital basis obtained from the cc-pVDZ atomic basis (see Ref. [27]) at its equilibrium geometry, $d = 1.6788\text{\AA}$, corresponding to a full orbital space CAS(12,68) with $\dim \mathcal{H}_{\text{FCI}} \approx 5 \times 10^{16}$, is shown in Fig. 5. In the numerical calculations we have used $M_{\text{min}} = 2048$, $M_{\text{max}} = 10000$, $\chi = 10^{-6}$, $\epsilon_{\text{Davidson}} = 10^{-6}$ and eleven sweeps. Here, due to the large orbital space we do not have access to the full-CI energy, so we first perform our extrapolation scheme yielding the predicted parameters shown in Fig 5 (a) and (b). Next, using the predicted full-CI energy, $E_{\text{RAS-X}} = -2086.891$, we show in Fig. 5 (c) that the linear scaling on double logarithmic axes for different ℓ values is recovered, as expected. Comparing our result to CCSD, CCSD(T), CCSDT, and CCSDTQ ($E = -2086.7401$, -2086.8785 , -2086.8675 , -2086.8689 , respectively) we conclude that our data point $E^0(17, 2) = -2086.8769$ is already below the CCSDTQ by 8×10^{-3} , while the extrapolated energy is between $E_{\text{RAS-X}} = 2086.884$ ($p_{\text{RAS-X}} = 2.06$) and $E_{\text{RAS-X}} = 2086.891$ ($p_{\text{RAS-X}} = 1.88$) using the first 12 or 14 data points in the fit, leading to an error estimate of the order of 10^{-3} . We have excluded the last three data points from the fit ($\ell = 15, 16, 17$) since the dynamically selected DMRG bond dimension has hit the upper threshold M_{max} .

Next, we analyze the stability of the extrapolation with respect to the accuracy threshold imposed on DMRG. Lowering the accuracy, i.e., using $\chi = 10^{-4}$, our data points for the largest ℓ values shifted upwards by the order of 10^{-3} and we obtained $E_{\text{RAS-X}} = -2086.881$ with $p_{\text{RAS-X}} = 2.08$. Increasing the value of χ further to 10^{-3} we obtained $E^0(14, 2) = -2086.8599$ with $\max(M) \simeq 4000$ only, and the extrapolation yielded $E_{\text{RAS-X}} = -2086.873$ with $p_{\text{RAS-X}} = 2.02$. Therefore, DMRG-RAS-X even with limited accuracy, i.e., with limited computational demands, can provide a better and hence a more accurate energy than the high rank CCSDTQ coupled cluster approach. That $E_{\text{RAS-X}}$ with $\chi = 10^{-4}$ is more accurate here than E_{CCSDTQ} follows from the fact that $E_{\text{CCSDTQ}} > E_{\text{RAS-X}}(\chi = 10^{-4}) > E^0(17, 2) > E_{\text{FCI}}$.

Finally we discuss results for the dicarbon molecule, but for the significantly larger cc-pVQZ basis set with frozen cores for $d = 1.25\text{\AA}$ corresponding to CAS(8,108) with $\dim \mathcal{H}_{\text{FCI}} \approx 1 \times 10^{14}$. See Fig. 6. Our extrapolation procedure yields $p_{\text{RAS-X}} = 3.48$ and $E_{\text{RAS-X}} = -75.803$

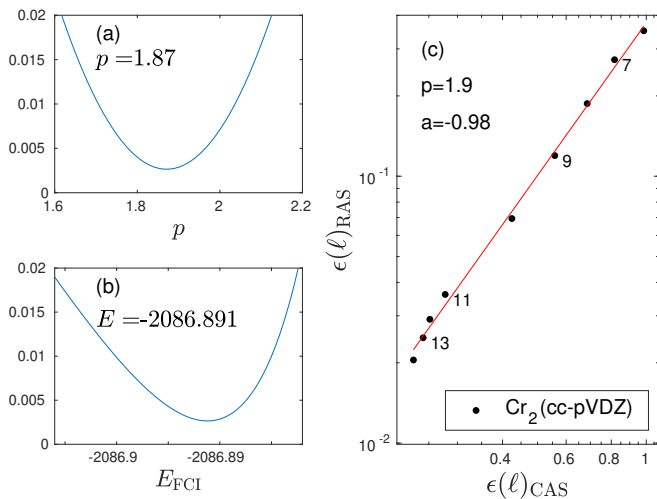


FIG. 5. Similar to Fig. 2, but for the chromium dimer at its equilibrium geometry, $d = 1.6788\text{\AA}$ in a natural orbital basis obtained from the cc-pVDZ atomic basis, corresponding to a full orbital space CAS(12,68). Here, first the extrapolation has been performed to obtain the predicted exponent $p_{\text{RAS-X}}$ and energy value $E_{\text{RAS-X}}$ as shown in panel (a) and (b), and the predicted energy was used to get the curve presented in panel (c).

using $\ell = 4 \dots 14$. Note that the error of the bare $E(14, 2) = -75.7971$ is 3.6×10^{-3} with respect to the $E_{\text{CCSD(T)}} = -75.8007$ reference value. Again the linear trend seen in Fig. 6(c) using $p_{\text{RAS-X}}$ and $E_{\text{RAS-X}}$ confirms the theory even for very large basis sets.

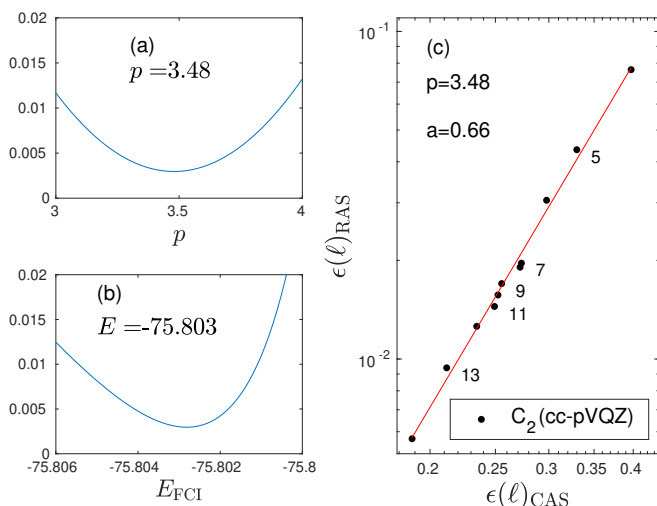


FIG. 6. Similar to Fig. 5, but for the significantly larger cc-pVQZ basis set with frozen cores for $d = 1.25\text{\AA}$, corresponding to CAS(8,108). In the extrapolation procedure we have used $\ell = 4 \dots 14$.

V. CONCLUSIONS AND OUTLOOK

In this work, we have presented a careful theoretical analysis of the DMRG-RAS method and introduced a parameter-free extrapolation method to predict the ground state energy within chemical accuracy for challenging strongly correlated systems and large basis sets. The theoretical analysis and the extrapolation method were validated by large scale numerical simulations.

(a) We have shown that DMRG-RAS is an embedding method which accounts for forward and backward scattering between the CAS and the EXT (RAS) orbital spaces, unlike previous post-DMRG approaches like perturbation theory or tailored coupled cluster. We also showed that the method is variational, providing an upper bound on the true energy.

(b) We have derived a power law error scaling which relates the bare CAS energy and the DMRG-RAS energy as the CAS size is varied, for weak interactions and for general systems. Such a power law makes DMRG-RAS superior to other methods such as DMRG-TCC where errors are not even monotone. Based on the theory we introduced a new extrapolation method, dubbed DMRG-RAS-X, that is argued to provide the ground state energy within chemical accuracy for large systems as well. Moreover the difference between the DMRG-RAS and DMRG-RAS-X energy provides a useful intrinsic estimate of the DMRG-RAS error.

(c) We have numerically justified the validity of the power law error scaling for various small and large systems possessing single and multi reference characters, using full-CI reference energies from the literature or provided by large scale DMRG calculations on the full orbital space. We have also demonstrated that the absolute error is reduced significantly by the new extrapolation method, with better and better error reduction as the fraction of RAS orbitals increases, as inevitably happens for large systems.

(d) We have applied DMRG-RAS-X to obtain new benchmark predictions of the full-CI ground state energy for the chromium dimer and for the dicarbon using very large basis sets, which improve on previous high excitation rank coupled cluster reference data.

The DMRG-RAS method is variational, free of uncontrolled errors, and – together with the new extrapolation method, the DMRG-RAS-X – very robust, achieving chemical accuracy with limited computational demands. These unique properties make DMRG-RAS-X a vital alternative method for electronic structure calculations.

Extension of our analysis for ground and excited states in strongly correlated molecular clusters and to higher dimensional quantum lattice models via the fermionic mode optimization [35, 36, 62] is under progress.

ACKNOWLEDGMENTS

Ö.L. has been supported by the Hungarian National Research, Development and Innovation Office (NKFIH) through Grant Nos. K134983 and TKP2021-NVA, by the Quantum Information National Laboratory of Hungary, and by the Hans Fischer Senior Fellowship programme funded by the Technical University of Munich – Institute for Advanced Study. G.B. acknowledges support

from NKFIH Grant No. FK-135496. The development of DMRG libraries has been supported by the Center for Scalable and Predictive methods for Excitation and Correlated phenomena (SPEC), funded as part of the Computational Chemical Sciences Program by the U.S. Department of Energy (DOE), Office of Science, Office of Basic Energy Sciences, Division of Chemical Sciences, Geosciences, and Biosciences at Pacific Northwest National Laboratory.

-
- [1] M. Swart and M. Gruden, *Accounts of Chemical Research* **49**, 2690 (2016), pMID: 27993008.
- [2] A. Khedkar and M. Roemelt, *Phys. Chem. Chem. Phys.* **23**, 17097 (2021).
- [3] M. Feldt and Q. M. Phung, *European Journal of Inorganic Chemistry* **2022**, e202200014.
- [4] D. Pantazis, M. Orio, T. Petrenko, S. Zein, E. Bill, W. Lubitz, J. Messinger, and F. Neese, *Chemistry – A European Journal* **15**, 5108.
- [5] S. Sharma, K. Sivalingam, F. Neese, and G. K.-L. Chan, *Nature Chemistry* **6**, 927 (2014).
- [6] D. J. Vinyard and G. W. Brudvig, *Annual Review of Physical Chemistry* **68**, 101 (2017), pMID: 28226223.
- [7] W. Lubitz, M. Chrysin, and N. Cox, *Photosynthesis Research* **142**, 105 (2019).
- [8] A. Kerridge, “The complete-active-space self-consistent-field approach and its application to molecular complexes of the f-elements,” in *Computational Methods in Lanthanide and Actinide Chemistry* (John Wiley and Sons, Ltd) Chap. 5, pp. 121–146.
- [9] M. Spivak, K. D. Vogiatzis, C. J. Cramer, C. d. Graaf, and L. Gagliardi, *The Journal of Physical Chemistry A* **121**, 1726 (2017), pMID: 28128563.
- [10] C. A. Gaggioli and L. Gagliardi, *Inorganic Chemistry* **57**, 8098 (2018), <https://doi.org/10.1021/acs.inorgchem.8b00170>.
- [11] T. Saue, *ChemPhysChem* **12**, 3077.
- [12] P. Pyykkö, *Annual review of physical chemistry* **63**, 45 (2012).
- [13] M. Reiher and A. Wolf, “Special computational techniques,” in *Relativistic Quantum Chemistry* (John Wiley and Sons, Ltd) Chap. 14, pp. 527–566.
- [14] P. Tecmer, K. Boguslawski, and D. Kedziera, “Relativistic methods in computational quantum chemistry,” in *Handbook of Computational Chemistry*, edited by J. Leszczynski (Springer Netherlands, Dordrecht, 2016) pp. 1–43.
- [15] W. Liu, *The Journal of Chemical Physics* **152**, 180901 (2020), <https://doi.org/10.1063/5.0008432>.
- [16] A. D. Becke, *The Journal of Chemical Physics* **138**, 074109 (2013).
- [17] C. L. Benavides-Riveros, N. N. Lathiotakis, and M. A. L. Marques, *Phys. Chem. Chem. Phys.* **19**, 12655 (2017).
- [18] P. Å. Malmqvist, A. Rendell, and B. O. Roos, *Journal of Physical Chemistry* **94**, 5477 (1990).
- [19] F. Jensen, “Introduction to computational chemistry,” (John Wiley and Sons, Inc., Hoboken, NJ, USA, 2006).
- [20] P. A. Malmqvist, K. Pierloot, A. R. M. Shahi, C. J. Cramer, and L. Gagliardi, *The Journal of Chemical Physics* **128**, 204109 (2008).
- [21] H. Lischka, D. Nachtigallova, A. J. A. Aquino, P. G. Szalay, F. Plasser, F. B. C. Machado, and M. Barbatti, *Chemical Reviews* **118**, 7293 (2018).
- [22] D. Casanova, *WIREs Computational Molecular Science* **12**, e1561.
- [23] S. R. White, *Phys. Rev. Lett.* **69**, 2863 (1992).
- [24] S. R. White and R. L. Martin, *The Journal of Chemical Physics* **110**, 4127 (1999), <https://doi.org/10.1063/1.478295>.
- [25] Ö. Legeza and J. Sólyom, *Phys. Rev. B* **68**, 195116 (2003).
- [26] G. Barcza, Ö. Legeza, K. H. Marti, and M. Reiher, *Phys. Rev. A* **83**, 012508 (2011).
- [27] G. Barcza, M. A. Werner, G. Zaránd, Ö. Legeza, and T. Szilvási, “Towards large-scale restricted active space calculations inspired by the schmidt decomposition,” (2021).
- [28] T. Kinoshita, O. Hino, and R. J. Bartlett, *The Journal of Chemical Physics* **123**, 074106 (2005), <https://doi.org/10.1063/1.2000251>.
- [29] R. J. Bartlett and M. Musiał, *Rev. Mod. Phys.* **79**, 291 (2007).
- [30] F. A. Evangelista, *The Journal of Chemical Physics* **149**, 030901 (2018), <https://doi.org/10.1063/1.5039496>.
- [31] P. Pulay, *International Journal of Quantum Chemistry* **111**, 3273.
- [32] Ö. Legeza and C. Schilling, *Phys. Rev. A* **97**, 052105 (2018).
- [33] I. Shapir, A. Hamo, S. Pecker, C. P. Moca, Ö. Legeza, G. Zarand, and S. Ilani, *Science* **364**, 870 (2019).
- [34] C. P. Moca, W. Izumida, B. Dóra, Ö. Legeza, J. K. Asbóth, and G. Zaránd, *Phys. Rev. Lett.* **125**, 056401 (2020).
- [35] C. Krumnow, L. Veis, Ö. Legeza, and J. Eisert, *Phys. Rev. Lett.* **117**, 210402 (2016).
- [36] C. Krumnow, L. Veis, J. Eisert, and Ö. Legeza, *Phys. Rev. B* **104**, 075137 (2021).
- [37] P. Piecuch, R. Tobol/a, and J. Paldus, *Phys. Rev. A* **54**, 1210 (1996).
- [38] L. Veis, A. Antalík, J. Brabec, F. Neese, Ö. Legeza, and J. Pittner, *The Journal of Physical Chemistry Letters* **7**, 4072 (2016).
- [39] A. Leszczyk, M. Máté, Ö. Legeza, and K. Boguslawski, “Assessing the accuracy of tailored coupled cluster methods corrected by electronic wave functions of polynomial cost,” (2021).
- [40] Y. Kurashige and T. Yanai, *The Journal of Chemical Physics* **135**, 094104 (2011).

- [41] Y. Kurashige, G. K.-L. Chan, and T. Yanai, *Nature Chemistry* **5**, 660 (2013).
- [42] S. Sharma and G. K.-L. Chan, *The Journal of Chemical Physics* **141**, 111101 (2014), <https://doi.org/10.1063/1.4895977>.
- [43] M. Saitow, Y. Kurashige, and T. Yanai, *The Journal of Chemical Physics* **139**, 044118 (2013).
- [44] Y. Cheng, Z. Xie, and H. Ma, *The Journal of Physical Chemistry Letters* **13**, 904 (2022), pMID: 35049302, <https://doi.org/10.1021/acs.jpcllett.1c04078>.
- [45] F. M. Faulstich, A. Laestadius, Ö. Legeza, R. Schneider, and S. Kvaal, *SIAM Journal on Numerical Analysis* **57**, 2579 (2019).
- [46] F. M. Faulstich, M. Mate, A. Laestadius, M. A. Csirik, L. Veis, A. Antalík, J. Brabec, R. Schneider, J. Pittner, S. Kvaal, and Ö. Legeza, *Journal of Chemical Theory and Computation* **15**, 2206 (2019).
- [47] Sz. Szalay, M. Pfeffer, V. Murg, G. Barcza, F. Verstraete, R. Schneider, and Ö. Legeza, *Int. J. Quantum Chem.* **115**, 1342 (2015).
- [48] C. J. Cramer, M. Włoch, P. Piecuch, C. Puzzarini, and L. Gagliardi, *The Journal of Physical Chemistry A* **110**, 1991 (2006), pMID: 16451035, <http://dx.doi.org/10.1021/jp056791e>.
- [49] Y. Kurashige and T. Yanai, *The Journal of Chemical Physics* **130**, 234114 (2009).
- [50] G. K.-L. Chan, *Wiley Interdisciplinary Reviews: Computational Molecular Science* **2**, 907 (2012).
- [51] A. Baiardi and M. Reiher, *The Journal of Chemical Physics* **152**, 040903 (2020).
- [52] J. Dukelsky and S. Pittel, *Reports on Progress in Physics* **67**, 513 (2004).
- [53] Ö. Legeza, L. Veis, A. Poves, and J. Dukelsky, *Phys. Rev. C* **92**, 051303 (2015).
- [54] A. Tichai, S. Knecht, A. T. Kruppa, Ö. Legeza, C. P. Moca, A. Schwenk, M. A. Werner, and G. Zarand, “Combining the in-medium similarity renormalization group with the density matrix renormalization group: Shell structure and information entropy,” (2022).
- [55] U. Schollwöck, *Rev. Mod. Phys.* **77**, 259 (2005).
- [56] R. Orús, *Annals of Physics* **349**, 117 (2014).
- [57] B.-X. Zheng, C.-M. Chung, P. Corboz, G. Ehlers, M.-P. Qin, R. M. Noack, H. Shi, S. R. White, S. Zhang, and G. K.-L. Chan, *Science* **358**, 1155 (2017).
- [58] H. R. Larsson, H. Zhai, K. Gunst, and G. K.-L. Chan, (2021), arXiv:2109.11036.
- [59] O. Legeza, J. Röder, and B. A. Hess, *Phys. Rev. B* **67**, 125114 (2003).
- [60] Ö. Legeza and J. Sólyom, *Phys. Rev. B* **70**, 205118 (2004).
- [61] A. Szabo and N. S. Ostlund, “Modern quantum chemistry: Introduction to advanced electronic structure theory,” (Dover Publications, Inc., Mineola, New York, 1996).
- [62] M. Máté, K. Petrov, S. Szalay, and Ö. Legeza, *Journal of Mathematical Chemistry* (2022), 10.1007/s10910-022-01379-y.
- [63] C. J. Stein and M. Reiher, *J. Chem. Theory Comput.* **12**, 1760 (2016).
- [64] A. Schafer and R. Horn, Hans and Ahlrichs, *The Journal of Chemical Physics* **97**, 2571 (1992).
- [65] T. H. Dunning, *The Journal of Chemical Physics* **90**, 1007 (1989), <https://doi.org/10.1063/1.456153> [doi.org].
- [66] Y. Ma, S. Knecht, S. Keller, and M. Reiher, *Journal of Chemical Theory and Computation* **13**, 2533 (2017), pMID: 28485978.
- [67] S. Sharma and G. K.-L. Chan, *The Journal of Chemical Physics* **136**, 124121 (2012), <https://doi.org/10.1063/1.3695642>.
- [68] H. R. Larsson, H. Zhai, C. J. Umrigar, and G. K.-L. Chan, *Journal of the American Chemical Society* **144**, 15932 (2022), pMID: 36001866.